KLOE Note 214
November 2006

$\phi \to \eta^{'} \gamma$ in $\pi^+\pi^-$ 7γ at KLOE

Camilla Di Donato
Universitá e Sezione INFN, Napoli

Abstract

We present the analysis of $\phi \to \eta' \gamma$ in $\pi^+\pi^-$ seven γ, using the data sample collected in the years 2001-2002, for an integrated luminosity of 427 pb^{-1}, run numbers 17874-26965. The selection criteria, and study of systematic effects, are described.

We measured the $R_\phi = BR(\phi \to \eta'\gamma)/BR(\phi \to \eta\gamma) = (4.77 \pm 0.09 \pm 0.19) \cdot 10^{-3}$ from which we derive BR$(\phi \to \eta'\gamma) = (6.20 \pm 0.11 \pm 0.25) \cdot 10^{-5}$ and the pseudo-scalar mixing angle in the flavor basis in the hypotheses of no gluonium as $\varphi_P = (41.4 \pm 0.3_{\rm stat} \pm 0.7_{\rm sys} \pm 0.6_{\rm th})^\circ$.
Combining our result about R with other constraints, we evaluate the gluonium content of η' meson as $Z^2 = 0.14 \pm 0.04$ and the mixing angle $\varphi_P = (39.7 \pm 0.7)^\circ$.

Introduction

The value of the $\eta - \eta'$ mixing angle in the pseudo-scalar meson nonet, θ_P, has been discussed many times in the last thirty-five years, and it become one of the most interesting SU(3)-breaking hadronic parameters to measure. In the context of Chiral Perturbation Theory [1] has been demonstrated that a description of the $\eta - \eta'$ system beyond leading order cannot be achieved in terms of just one angle, but we need two parameters θ_8 and θ_0. If we express in the flavor basis the analogous parametrization, the two mixing parameters are φ_q and φ_s. The situation in the quark-flavor basis is different from the one in the octet-singlet one, the difference between the two angles, φ_q and φ_s, is determined by an OZI-rule violating contribution. The experimental numbers enter to give two mixing angles close one to the other in the quark-flavor basis: $|(\varphi_q - \varphi_s)/(\varphi_q + \varphi_s)| \ll 1$ and the difference between the two parameters can be neglected; this is not true for θ_8 and θ_0. If we choose the flavor basis the advantage is to deal with only one mixing angle $\varphi_P \simeq \varphi_q \simeq \varphi_s$ [2].

We study the $\phi \to \eta'\gamma$ decay because its branching ratio can probe the $|s\bar{s}>$ and gluonium content of the η' [3]. The ratio of the two branching ratio $\phi \to \eta'\gamma$ and $\phi \to \eta\gamma$ can be related to the $\eta - \eta'$ mixing angle in the flavor basis[4]. The best measurement available to date of $BR(\phi \to \eta'\gamma)$ has been published by KLOE [5], and has been obtained from the analysis of $\phi \to \eta'\gamma$ decay with $\pi^+\pi^-\gamma\gamma\gamma$ final state, based on an integrated luminosity of about $16pb^{-1}$, collected during year 2000. In the present work we show the measurement obtained using an integrated luminosity of $427pb^{-1}$, almost all the events collected in 2001 and 2002, with evaluation of systematic contribution to the branching ratio. Measuring the ratio $R = BR(\phi \to \eta'\gamma)/BR(\phi \to \eta\gamma)$ and using the approach by Bramon [4], as done in [6], we give the pseudo-scalar mixing angle in the flavor basis with a statistical error of 0.3°. The accuracy of the new measurement is better than the previous one.
In a previous memo [7] we described the absolute measurement of the branching ratio $\phi \to \eta'\gamma$ performed on a subsample of 2000 data, $16pb^{-1}$, with a first study of systematics; in the present analysis we start from the previous experience.

Let me remind you the decays under study: we are interested in the $\phi \to \eta'\gamma$ decay with two tracks and seven photons final state; we have to perform the inclusive measurement of the following decays:

- $\eta' \to \eta\pi^+\pi^-$ with $\eta \to \pi^0\pi^0\pi^0$ and $\pi^0 \to \gamma\gamma$;
  $BR_{crg} = (13.9 \pm 0.5)\%$ (charged channel)
- $\eta' \to \eta\pi^0\pi^0$ with $\eta \to \pi^+\pi^-\pi^0$ and $\pi^0 \to \gamma\gamma$;
  $BR_{ntr} = (4.6 \pm 0.3)\%$ (neutral channel)

The backgrounds are due to $\phi \rightarrow K_S K_L$[1]:

1. $K_S \rightarrow \pi^+\pi^-$ and $K_L \rightarrow \pi^0\pi^0\pi^0$
   $BR_1(\phi \rightarrow K_S K_L \rightarrow \pi^+\pi^- 6\gamma\text{'s}) = (4.8 \pm 0.1)\%$

2. $K_S \rightarrow \pi^0\pi^0$ and $K_L \rightarrow \pi^+\pi^-\pi^0$
   $BR_2(\phi \rightarrow K_S K_L \rightarrow \pi^+\pi^- 6\gamma\text{'s}) = (1.28 \pm 0.03)\%$

3. $K_S \rightarrow \gamma\pi^+\pi^-$ and $K_L \rightarrow \pi^0\pi^0\pi^0$
   $BR_3(\phi \rightarrow K_S K_L \rightarrow \gamma\pi^+\pi^- 7\gamma\text{'s}) = (3.36 \pm 0.10) \cdot 10^{-4}$

Other backgrounds are negligible.
In order to measure the ratio $R = BR(\phi \rightarrow \eta'\gamma)/BR(\phi \rightarrow \eta\gamma)$, we have to select also the $\phi \rightarrow \eta\gamma$ decay; we look at the fully neutral final state:

- $\phi \rightarrow \eta\gamma$
  - $\eta \rightarrow \pi^0\pi^0\pi^0$ with $\pi^0 \rightarrow \gamma\gamma$;

  $BR(\phi \rightarrow \eta\gamma \rightarrow 7\gamma) = (0.41 \pm 0.01)\%$

because it has topology very similar to the one of the η' decay a part the charged tracks. This η decay is essential background free; we use the general selection criteria as described in [9], plus some other features, we'll describe later.
In the next we will focus our attention on the η' analysis, because, except for the charged elements, the two decays have almost the same features.
In the first paragraph we describe the selection criteria for the η' analysis, starting from the first level selection, which is common to the two analysis and then we describe the topological selection and background suppression criteria; we show the experimental results for η' and give a background evaluation. The second paragraph shows the results for the η analysis, while the next one explain the systematic evaluation for both analysis. In the fourth section we evaluate the ratio between the two branching ratio and the statistical and systematic uncertainties. Finally in the last section we use our result to test possible gluonium content for the η'.

1 Analysis of η': study of the event selection

The events analyzed in the present work, has been collected in 2001 and 2002, and they were reconstructed and streamed using datarec version 13 and 14. They were selected by radiative stream to reduce background from neutral kaons, bhabha and cosmic ray events. The events of radiative stream are written on tape in DST-format in neutral radiative and charged one. This analysis has been performed on events selected as charged radiative events, for the $\phi \rightarrow \eta'\gamma$ and on events selected as neutral radiative ones for $\phi \rightarrow \eta\gamma$.
We use the official Monte-Carlo (MC) RAD04 to study the selection efficiency for the signals and the power rejection for background.
We have first level selection, due to the standard preselection of the events which is the same for all events in the same stream, and it consist of *Trigger (Trig), Filfo (Flf)* and *Event Classification (ECL)*; a second level selection where a dedicated selection filter is applied. A kinematic fit with constraints on photons and on quadrimomentum conservation is applied to all events.

1.1 Trigger, Filfo and Event Classification

The trigger efficiency is very high for both the channel that contribute to the final state under study. The efficiency are found to be 99.7% for the η' charged channel and 99.9% for the neutral one. The comparison of the trigger sector multiplicities from MC and the ones for real data shows a reasonable agreement (fig.1).

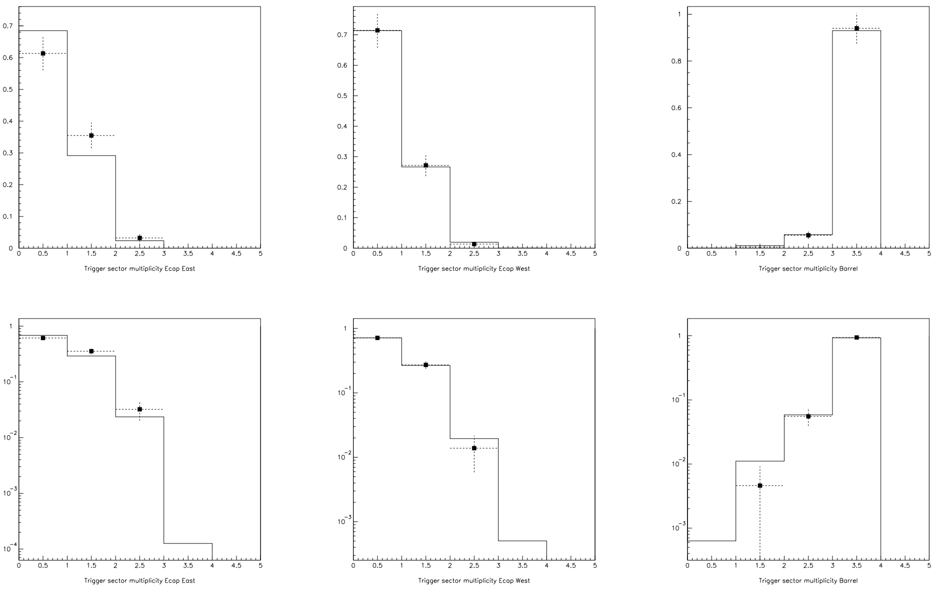

Figure 1: Trigger sector multiplicity; up: linear scale, down: log-scale

The overall inefficiency induced on the final analysis is very small in fact the trigger efficiency for events which pass the full analysis is high, 99.97% for the η' charged channel and 100% for the neutral one, then we will use trigger efficiency evaluated by MC neglecting systematics due to the trigger.

Filfo is the machine background filter and the it has a 100% efficiency for the triggered events for both the signal channels.

The Event Classification efficiency for triggered events, filtered by filfo, are 57.88% for the charged channel and 61.45% for the neutral one. The difference in EVCL efficiency between the two samples is due to the different charged vertex efficiency. The Event Classification efficiency for events which pass the full analysis is almost high; we have from MC study that the efficiency is 99.07% and 97,03% for charged and neutral channel, but we need to evaluate possible systematic bias introduced by the EVCL selection. This has been done analyzing a subsample of the data starting from raw and without EVCL selection; in the section 3 we will describe the results.

1.2 Topological selection and Background suppression

The final state of the decays analyzed is given by seven photons and two tracks coming out from a vertex. In the topological selection we ask for:

- one charged vertex in the cylindrical region:
  $0 < \rho_{vtx} < 4\ cm$ and $|z_{vtx}| < 8\ cm$
  with two opposite charged tracks;
- seven prompt neutral clusters with $E_\gamma > 10MeV$ over $21°$

A prompt neutral cluster is a cluster in the Electromagnetic Calorimeter which satisfies the condition[2] $|t_{clu} - r_{clu}/c| < min(5 \cdot \sigma_t, 2ns)$ and with no associated tracks coming from the Drift Chamber.

At this level we have selected two charged tracks connected with a vertex and seven neutral prompt clusters; we performed a kinematic fit imposing global energy-momentum conservation with the hypothesis that the clusters are produced by photons coming from the origin.

[1]The branching ratio for bg1 and bg2 are from PDG'04 value; about bg3 we use the value from [8], measured with $E_\gamma >$ 20MeV, as in our experiment, while the PDG one is obtained with to $E_\gamma >$ 50MeV

[2]The time window is limited by 2 ns to reduce the presence of accidental clusters.

We have a fit with 46 parameters and 11 constraints; the inputs are energy, position and time for each photons, which means five parameters per photons; position of charged vertex, three parameters; transverse momentum, $cot\theta$ and ϕ at the vertex for each tracks, three parameters per tracks; beam energies, two parameters. The kinematic fit is performed using a standard Lagrange multipliers technique.
After the fit we have an improvement on the resolutions and the χ^2 of the fit is a quality check of the imposed conditions. In fig.2 we show the χ^2/Ndf distribution for MC signal and what we find on data, after background suppression. A cut on $\chi^2/Ndf < 4.54$ for the fit is imposed to ensure the good reconstruction

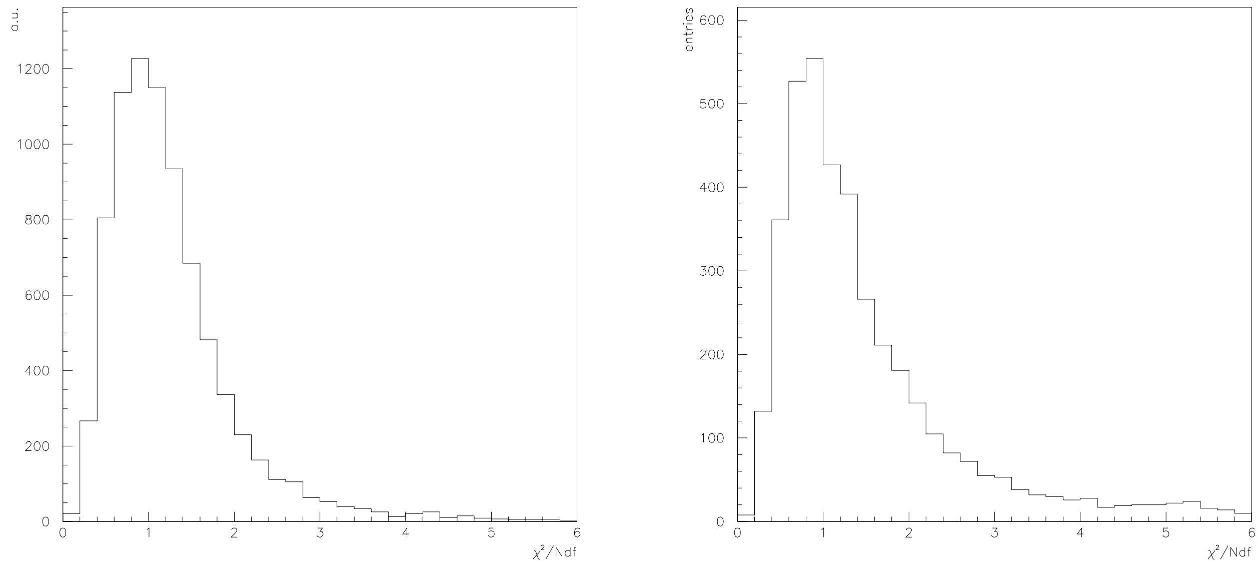

Figure 2: Reduced χ^2; left is MC only signal; right data

of the events. The χ^2/Ndf variable shows a reasonable agreement between data and MC, see fig.3.

In this section we study how to reject events, which can have or simulate the signal final state, but are produced by different decay. The energy distribution of prompt neutral clusters doesn't help to reject background, while charged information do, as you can see in [7].
The first cut to reduce the background make use of the event classification. Usually the streaming procedure assigns an events at least to one stream. Our events mainly fires radiative stream, then we choose to retain events written only in the radiative stream; the three backgrounds come from the neutral kaon stream. This cut, the *KtagVeto*, is very useful to reject bg1 and bg3, but doesn't help with bg2. This background can be rejected using the fact that it mimics the signal if there is an accidental clusters in time window or a split cluster; i.e. there is at least one low energy cluster. A cut on the energy of the cluster after kinematic fit reduce this background (fig.4): we ask for $E_{min} > 20MeV$.

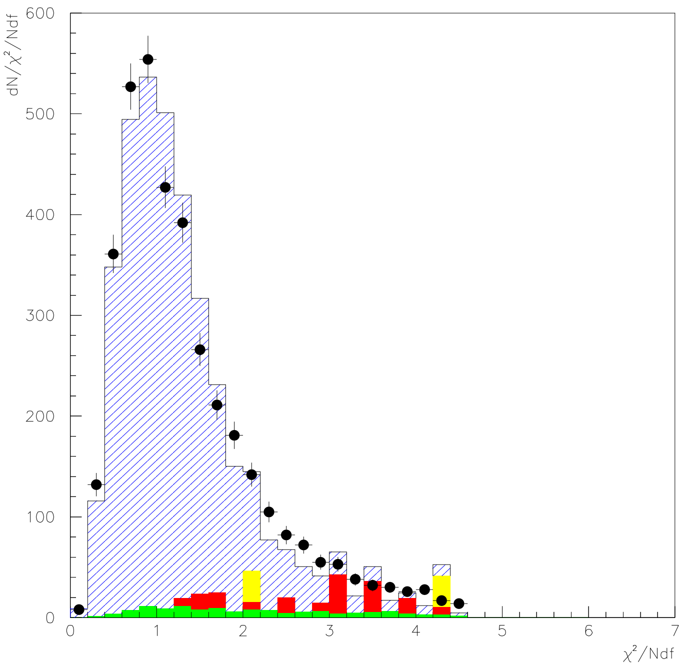

Figure 3: Reduced χ^2; bg1 *yellow*, bg2 *red*, bg3 *green*, line is MC signal plus all bg and dots are data

Finally from visual scan on data sample, done with the event display DIDONE (fig.5.left), we find background due to multi-photons final state events in which there is a production of a charged vertex and the two out coming tracks are parallel (fig.5.right); for this reason we cut away events in which $cos\theta_{\pi^+\pi^-} \geq 0.84$.
The signal full analysis, apart Flf-EVCL, can be translated in the overall selection efficiencies: $(23.45 \pm 0.16)\%$ to be combined with Filfo-EVCL efficiency measured on data 97%, as you can see from section.3. For background the overall power rejections are summaryzed in the table.1:

	bg1	bg2	bg3
BR	$(4.8 \pm 0.1)\%$	$(1.28 \pm 0.03)\%$	$(3.36 \pm 0.10)10^{-4}$
ε	$9 \cdot 10^{-7}$	$0.875 \cdot 10^{-5}$	$28 \cdot 10^{-5}$

Table 1: Branching ratio and fraction of background events which survey after the cuts

1.3 The η' events

Applying the full selection criteria described above to the data collected in 2001-2002, we find

$$N^{observed} = 3750 \pm 61; \tag{1}$$

The expected background from MC analysis is:

- $N^{bg1} = BR(bg1) \times \varepsilon^{bg1}_{MC} \times N^{\phi} = 59$
- $N^{bg2} = BR(bg2) \times \varepsilon^{bg2}_{MC} \times N^{\phi} = 155$
- $N^{bg3} = BR(bg3) \times \varepsilon^{bg3}_{MC} \times N^{\phi} = 131$

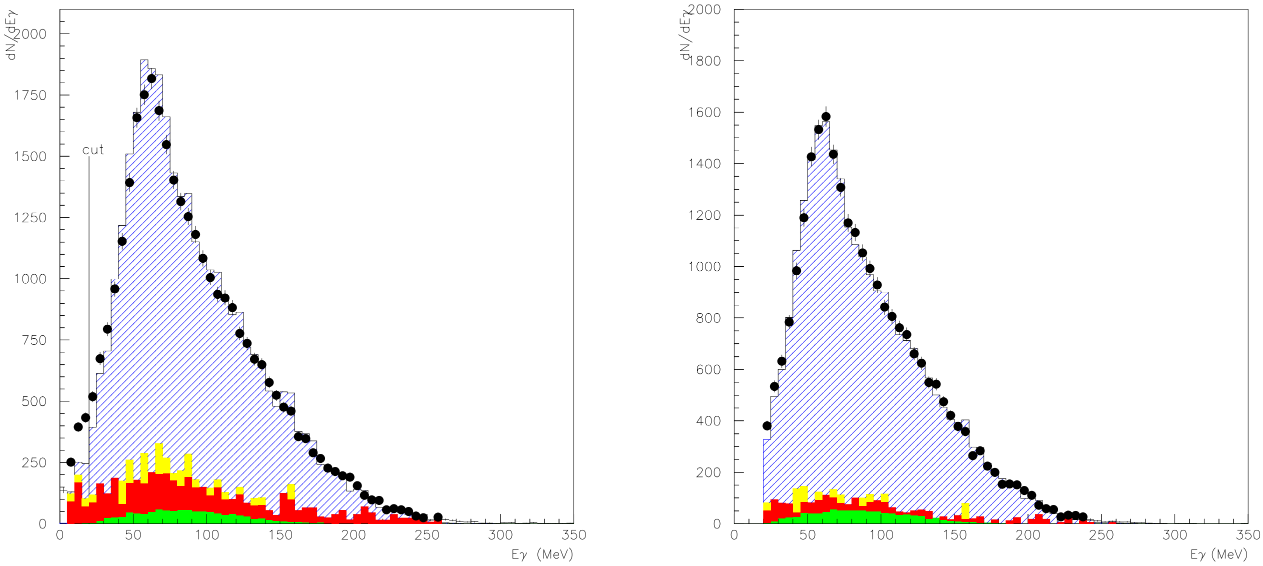

Figure 4: Energy distribution of all seven prompt neutral clusters, the plot on the left is before the cut on the energy of the less energetic cluster, the plot on the right is after the cut; bg1 *yellow*, bg2 *red*, bg3 *green*, line is MC signal plus all bg and dots are data

Finally we find

$$N^{\eta'\gamma} = 3405 \pm 61; \tag{2}$$

In the section 3 we will evaluate a systematic contribution due to the background subtraction.
One of the main problem in this analysis is that there is no way to solve the combinatorial between photons in order to build an η' invariant mass to characterize the signal. Indeed we need to single out the photon radiated by the ϕ, from the others produced by the η' decays. Figure.6 shows the MC distribution of prompt neutral clusters energy for the selected events with the two contributors: the energy of photon radiated by the ϕ, on the top, and the energy of the photons due to the η' decay. We didn't find any criteria to separate the radiative from the others.

We plot, for each event, seven invariant masses, one for each photon, in the hypothesis that the chosen photon is the radiated one and the others are due to the η' decay. In fig.7 the MC-DATA comparison is shown for the $M_{\pi^+\pi^-7\gamma}$ invariant masses, built one for each photon; the agreement is good. In fig.8.left the line is the overall contribution due to physical backgrounds plus combinatorial background from MC and dots are DATA; fig.8.right shows the comparison between the MC η' *right* invariant mass (the line) and the data η' invariant mass (dots), obtained subtracting from the all combinations the overall MC background.

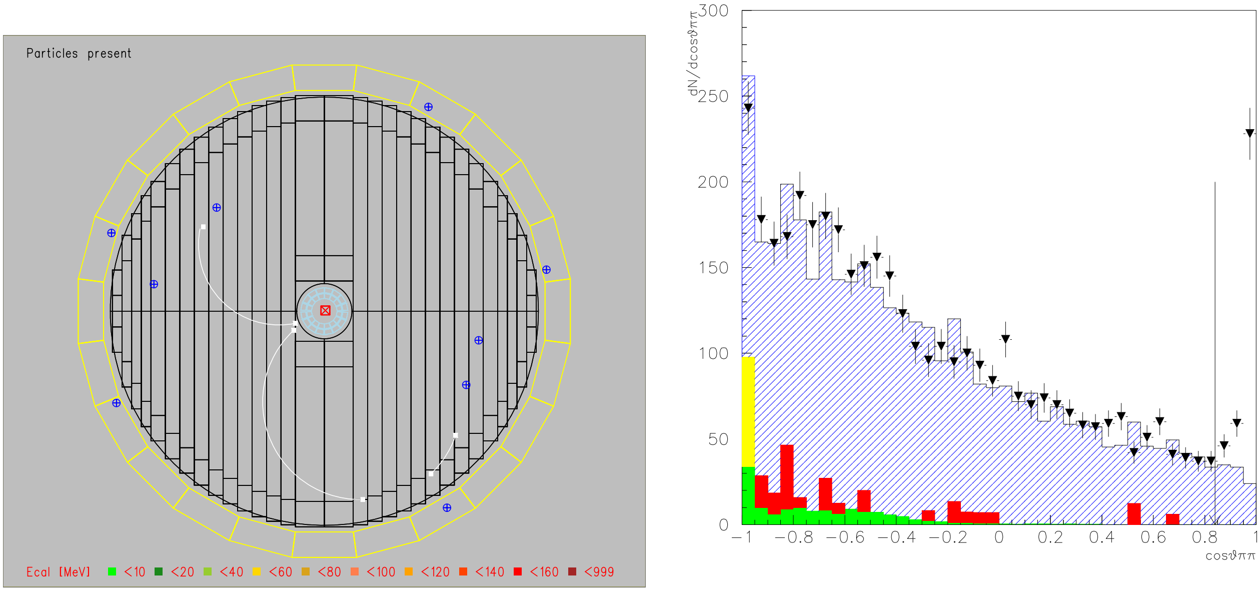

Figure 5: left: a sample of background events at $cos\theta_{\pi^+\pi^-} \sim 1$ with event display; right: Data-MC comparison for the cosine distribution of the angle between the two charged tracks; bg1 *yellow*, bg2 *red*, bg3 *green*, line is MC signal plus all bg and dots are data. Around cosine equal one we find on data events not predicted by MC; they are background due to multi photons final state events with two tracks due to photon-conversion

2 A normalization sample: the η decay

The same study has been done for the fully neutral final state. Again the trigger efficiency results to be very high. The Filfo-EVCL study performed on the minimum bias sample allow us to measure the efficiency for the analyzed events on data; the results is $(97.88 \pm 0.10)\%$ to be compared with the value from MC, $(99.27)\%$.

The topological selection adopted for the fully neutral final state is almost the same adopted for the previous one. We ask for

- seven prompt neutral clusters with $E_\gamma > 10 MeV$ over $21°$
- no tracks coming from the origin, to guarantee a neutral final state.

The mean features of the decay is the presence of a photon peaked at $365 MeV$, the one radiated by the ϕ, which is the most energetic one. We ask the most energetic photon was $320 MeV < E_\gamma < 400 MeV$. The remaining photons give the η invariant mass (fig.9.right). We apply a kinematic fit procedure with no mass constraint as for the η' decay; here we have 37 input parameters and 11 constraints. We use the selection done in [9], including the cuts used in the η' selection, related to cluster's informations, i.e. the cut on the minimum cluster energy and on the χ^2.
The selection efficiency from Monte-Carlo, without Filfo-EVCL, is 33.66%. Looking at the same sample used for the η' analysis we select

$$N^{\eta\gamma} = 1665000 \pm 1300 \tag{3}$$

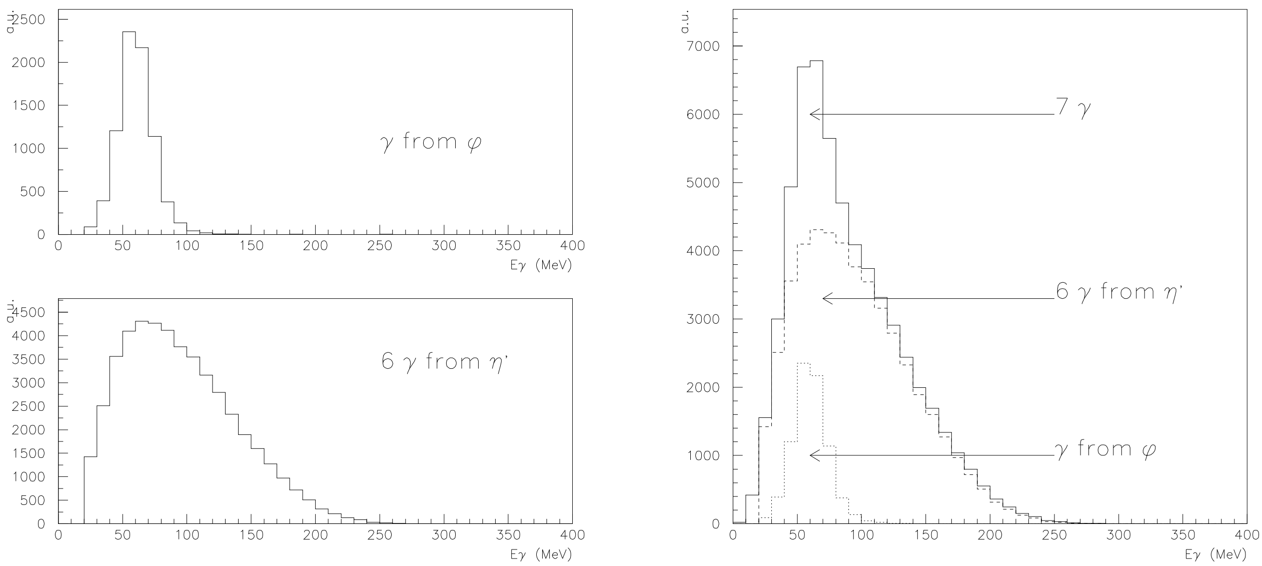

Figure 6: Distribution of E_γ from MC; on the left the two distribution for the γ radiated by the ϕ and the six γ's from the η' decay; on the right both contributions

3 The systematic checks

As described in the discussion about first level selection, we consider negligible systematics effect due to trigger selection.
The most important check regards the Event Classification. In order to check the systematic bias introduced by Filfo-EVCL, we have analyzed a subsample of the data without the two filters and we have evaluated the Filfo-EVCL efficiency on the events selected by this analysis, to compare the MC value with the real data one.
The raw data have been preselected without Filfo and EVCL, using very simple cuts [10], [11] and then reconstructed. The sample used has a luminosity of one tenth of the analyzed data and cover the full period under study. We have evaluated the discrepancy between data and MC for the selection efficiency of the combination Filfo-EVCL. Because the KtagVeto, in the η' analysis, use Event Classification information, we decide to evaluate the MC-data discrepancy in two different way: 1. in the standard analysis, we *forget* that KtagVeto use EVCL; 2. replacing the veto with a similar cut on the total energy associated to the charged pions, $E^{\pi^+} + E^{\pi^-} < 500$MeV. In both case we find for the ratio $R = BR(\phi \to \eta' \gamma)/BR(\phi \to \eta\gamma)$ a variation at level of 5 per mill: $\Delta R/R = 0.5\%$.
We decide to use this result as a correction and not as a systematics effect; so in the measurement we use the efficiency as evaluated from data. We define:

$$\varepsilon_{\eta'}^{Flf-EVCL} = \frac{BR_{crg} \times \varepsilon_{\eta'}^{Flf-EVCL}(crg) + BR_{ntr} \times \varepsilon_{\eta'}^{Flf-EVCL}(ntr)}{BR_{crg} + BR_{ntr}} \tag{4}$$

and we find on data the value 97%, to be compared with the MC one i.e. 98.50%.
The sample selected from raw produced $\sim 300 N_{events}$, this means that we measured the efficiency with an error of $\sim 1\%$; we can put it as a systematic contribution to the selection efficiency. The same has been done for the η channel and we find from data the efficiency value 97.88%, whose statistical error is negligible.

Systematics related to the tracking and vertexes regards only the η' selection; we use the $\phi \to \pi^+\pi^-\pi^0$ to check vertex efficiency. In fig.10.left the charged pion momentum for our signal is shown, while in fig.10.right

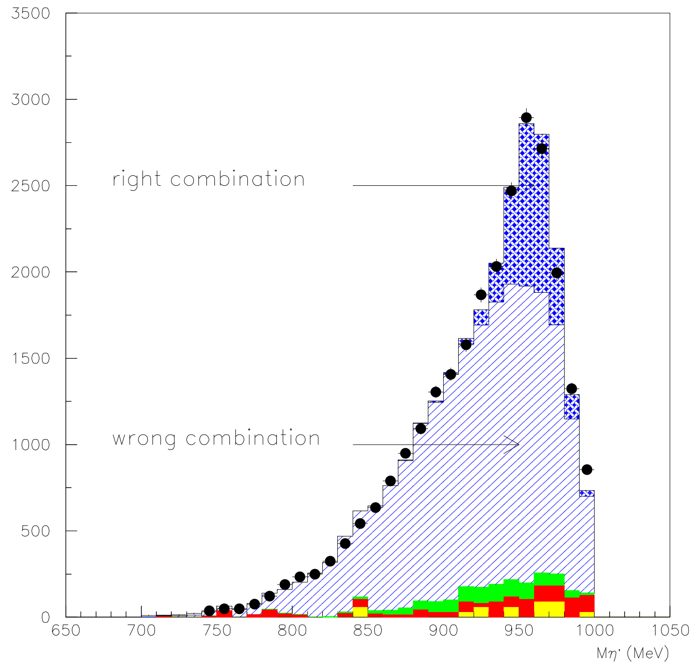

Figure 7: Distribution of $M_{\eta'}$; in *yellow* we have the background from bg1 , in *red* from bg2, in *green* from bg3; *bleu* is MC signal plus all bg, and we separated the MC signal in combinatorial background from wrong combinations and the signal from the right combination. Dots are data

you can see the same distribution for $\phi \to \pi^+\pi^-\pi^0$.

The $\phi \to \pi^+\pi^-\pi^0$ decay is very useful for this kind of study, because it cover the momentum range under study. We look for events characterized by two tracks in the chamber with momentum $50MeV < P < 400MeV$ and two prompt neutral clusters over $25°$, We ask for $|M_{\gamma\gamma} - M_{\pi}| < 20MeV$ and $850MeV < Ene_{TOT} < 1200MeV$ for the total energy. The background contamination is at level of 1.5%.

We studied the vertex efficiency as function of the minimum pion momentum; in fig.11-left we compare the MC vertex efficiency with the one on DATA. From the fit with a constant in the range $50MeV : 250MeV$, we found $\varepsilon^{VTX}_{DATA}/\varepsilon^{VTX}_{MC} = 0.99$, see fig.11-right.

The same has been done for the track efficiency, with additional cuts. We ask for other two clusters in the calorimeter, with at least $100MeV$ and $0.8 < \beta < 0.95$, in this way we close the event. We study the efficiency for a single track, so we ask at least one track in the DC with $200MeV < P < 400MeV$. Using this track and the two prompt neutral clusters we built the missing momentum. We look for a second track in a cone of $35°$ around the direction of the missing momentum. In fig.12-left we compare the MC track efficiency with the one on DATA. From the fit with a constant in the range $50MeV : 250MeV$, we found $\varepsilon^{TRK}_{DATA}/\varepsilon^{TRK}_{MC} = 0.99$, see fig.12-right.

We check the momentum distribution for the charged pions for our signal; see fig.13 for the P_T and P_Z distribution of the two charged tracks. In fig.14 the MC-DATA comparison on ρ charged vertex position is shown.

We studied the behavior of efficiency due to a variation of angular cut in the topological selection and of cut to the minimum cluster energy for the ratio of the two channels, in order to check the Monte-Carlo stability; the results are summarized in tab.2.

The uncertainty on the cut, due to the tail of the χ^2/Ndf distributions, is not trivial to evaluate, but an estimation of this effect can be obtained moving the cut and evaluating the maximum variation of the ratio $(\Delta\frac{N}{\varepsilon})/(\frac{N}{\varepsilon})$; we move the cut of an amount equal to one σ of the χ^2/Ndf distributions which means $\pm 20\%$

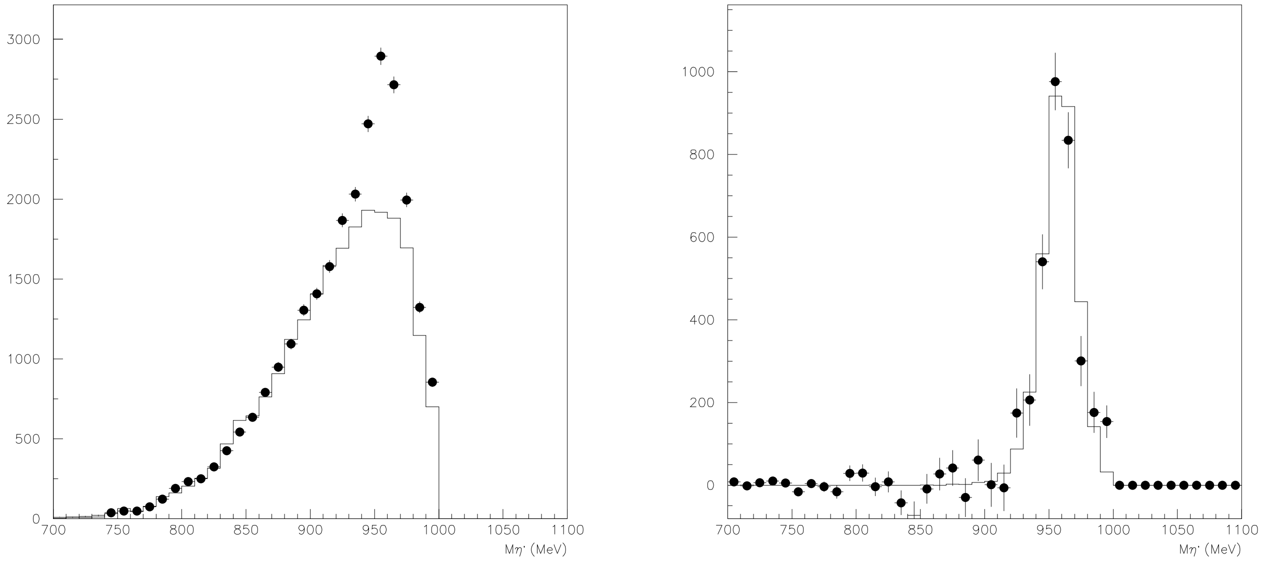

Figure 8: Distribution of $M_{\eta'}$. Left: dots are data, line are all background plus the wrong combination for signal. Right: dots are data, obtained subtracting from the all combination the MC background due both to physical background both to combinatorial background, line is MC right $M_{\eta'}$ for the signal.

check	$\Delta\varepsilon\eta$	$\Delta\varepsilon\eta'$	$\Delta(\varepsilon\eta/\varepsilon\eta')$	%
$\Delta\theta_\gamma = +1°$	-1.32%	-0.99%	$+0.006$	0.4%
$\Delta E_\gamma = \mp 2\%$	$^{+0.14\%}_{-0.16\%}$	$^{+0.07\%}_{-0.11\%}$	± 0.002	0.14%
TOTAL				0.4%

Table 2: Systematic checks about the ratio R; Monte-Carlo stability of common analysis efficiency ratio. $\varepsilon\eta/\varepsilon\eta' = 1.43$

of the cut, and we observe a maximum variation on R equal to 1.5%.
Another check regards the background. The background rejection study required an huge amount of MC events, this has been done with an ad hoc production. On the other hand we have the MC production with the simulation of right run conditions[3]. In order to evaluate systematics due to background subtraction, we compare results from official MC w.r.t. the ad hoc production. For the official MC we use dtr_stream_code='mrc' and mc_mccard_code='all_phys'. We find the following results: from the official MC we found that background due to the neutral kaon decays is at level of 8.5%, while, from the ad hoc production we evaluate a background at level of 9.2%; comparing these two numbers we can evaluate a systematic on the background subtraction: the background evaluated from MC is at level of $9.2 \pm 0.7\%$.
We have $345 \pm 6_{stat} \pm 28_{sys}$ background events.

[3]In the rad04 production we weighted the clusters using the Miscetti corrections optimized to solve a software bug problem [12]

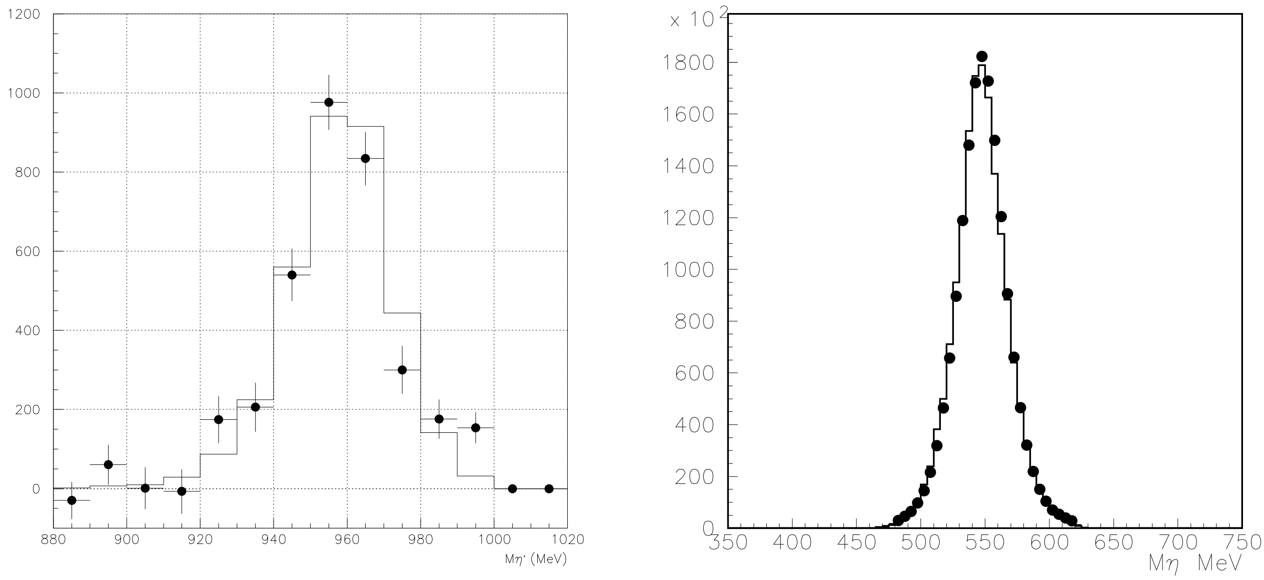

Figure 9: left: Distribution of $M_{\eta'}$, MC-DATA comparison from fig.8.right zoom ; right: Distribution of M_η

4 Results

The BR($\phi \to \eta^{'}\gamma$) will be evaluated using the decay $\phi \to \eta\gamma$ with $\eta \to 3\pi^0$ and $\pi^0 \to \gamma\gamma$ for normalization; first we have to determine the ratio $R = BR(\phi \to \eta^{'}\gamma)/BR(\phi \to \eta\gamma)$:

$$R = \frac{N_{\eta'\gamma}}{N_{\eta\gamma}} \frac{\varepsilon^{\eta}_{MC} \cdot \varepsilon^{\eta}_{data}}{\varepsilon^{\eta'}_{MC} \cdot \varepsilon^{\eta'}_{data}} \cdot \frac{\mathrm{BR}_{\eta\gamma}}{\mathrm{BR}_{\eta'\gamma}} \cdot K_\rho \tag{5}$$

where $\mathrm{BR}_{\eta\gamma}$ is the branching ratio $\mathrm{BR}(\eta \to 3\pi^0)$; $\mathrm{BR}_{\eta'\gamma}$ is $[\mathrm{BR}(\eta' \to \pi^+\pi^-\eta) \cdot \mathrm{BR}(\eta \to 3\pi^0) + \mathrm{BR}(\eta' \to \pi^0\pi^0\eta) \cdot \mathrm{BR}(\eta \to \pi^+\pi^-\pi^0)]$; both are multiplied by $\mathrm{BR}^3(\pi^0 \to \gamma\gamma)$, that will be cancel out in the ratio; $\varepsilon^{\eta'}_{MC}$ and ε^{η}_{MC} are the overall selection efficiency evaluated on MC, on sample selected without Filfo-EVCL filter; $\varepsilon^{\eta'}_{data}$ and $\varepsilon^{\eta}_{data}$ are the Filfo-EVCL filter efficiency measured on data.
The factor K_ρ accounts for interference between the amplitudes $A(\phi \to \eta(\eta')\gamma)$ and $A(\rho \to \eta(\eta')\gamma)$ evaluated in the Born approximation [6] and also for radiative corrections [15]. The correction depends from the $\sqrt{s}$; in the fig. 15 the $\sqrt{s}$ versus run numbers for 2001-2002 is shown. We evaluate the correction due to interference, for each run; see the fig. 16.
Instead to apply a run per run correction, we choose to correct with the mean value, weighted with run luminosity, and to use the standard deviation as systematic. In the range of $\sqrt{s}$ exploited, corrections at the cross section, due to the evaluation of radiative corrections are at level of 1% and we take in to account them and the final correction becomes $K_\rho = 0.94(\text{inter.}) * 1.01(\text{radiat.}) = 0.95$.

Evaluating the formula, using the following value for the involved quantity:

- $N_{\eta'\gamma} = 3405 \pm 61_{\text{stat}} \pm 28_{\text{sys}}$ and $N_{\eta\gamma} = 1665000 \pm 1300$;
- $(\varepsilon^{\eta}_{MC} \cdot \mathrm{BR}_{\eta\gamma})/(\varepsilon^{\eta'}_{MC} \cdot \mathrm{BR}_{\eta'\gamma}) = (2.43 \pm 0.09_{\text{syst.}})$
$\Longrightarrow 3.7\%$ (TRK$\oplus$VTX$\oplus\chi^2/Ndf\oplus$BR");
- $\varepsilon^{\eta}_{data}/\varepsilon^{\eta'}_{data} = 1.01 \pm 0.01 \Longrightarrow 1\%$;
- $K_\rho = 0.95 \pm 0.01 \Longrightarrow 1\%$.

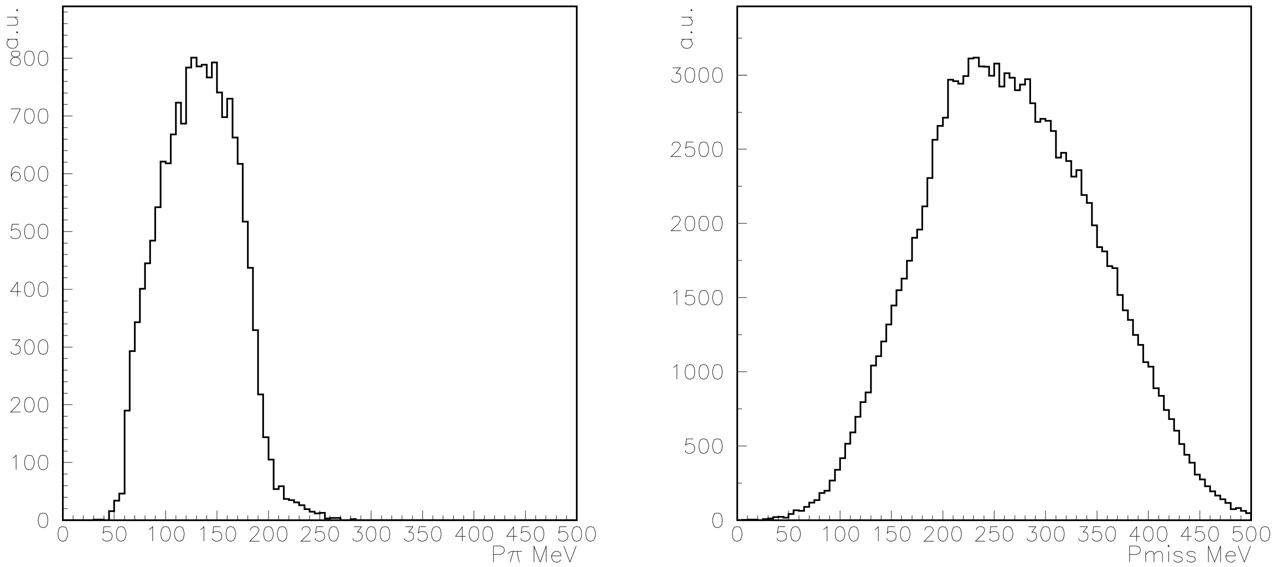

Figure 10: left: MC distribution of charged pion momentum for the signal; right: MC distribution of charged pion momentum for the control sample

we find

$$R = (4.77 \pm 0.09_{\rm stat} \pm 0.19_{\rm sys}) \cdot 10^{-3} \qquad (6)$$

The systematic errors comes out from the contribution as in table 3.

source	Syst. err.
EVCL	1%
TRK	1%
VTX	1%
BG	0.1%
$\varepsilon^{\eta\gamma}_{MC}/\varepsilon^{\eta'\gamma}_{MC}$	0.4%
χ^2/Ndf	1.5%
K_ρ	1%
BR"	3%
Total	4%

Table 3: Systematic contribution to the error on the ratio R

We use the BR($\phi \to \eta\gamma$)= $(1.301 \pm 0.024)\%$ as from [17] and finally we find:

$$\mathrm{BR}(\phi \to \eta'\gamma) = (6.20 \pm 0.11_{\rm stat} \pm 0.25_{\rm sys}) \cdot 10^{-5} \qquad (7)$$

We are compatible with our published value obtained with $16pb^{-1}$, $R = (4.70 \pm 0.47_{\rm stat} \pm 0.31_{\rm sys}) \cdot 10^{-3}$ and $\mathrm{BR}(\phi \to \eta'\gamma) = (6.10 \pm 0.61_{\rm stat} \pm 0.43_{\rm sys}) \cdot 10^{-5}$ ref.[5].

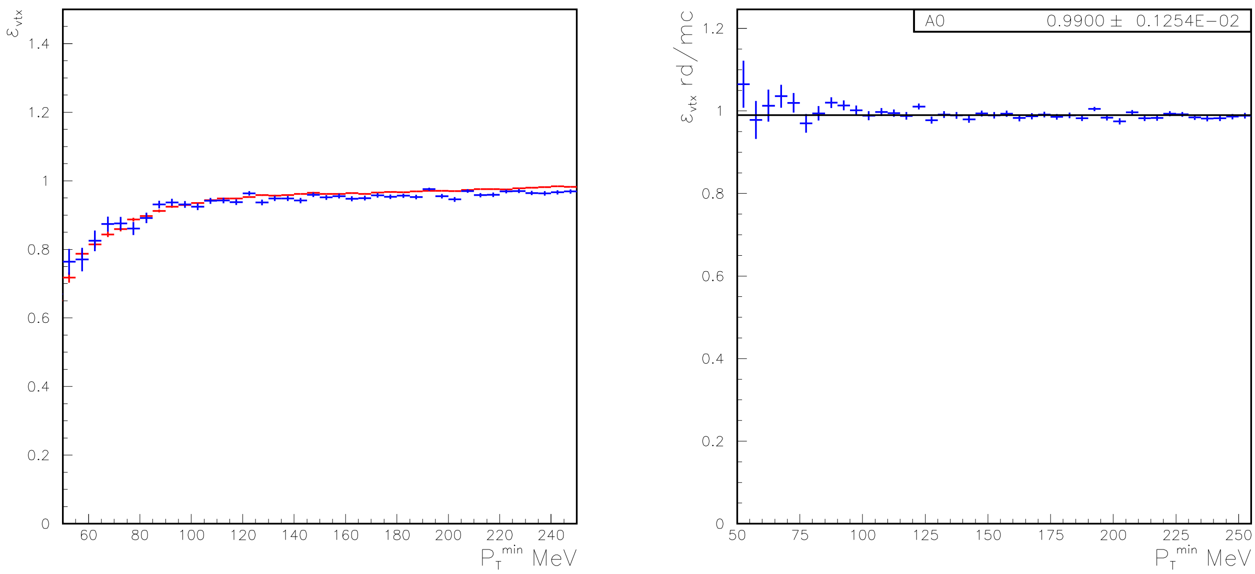

Figure 11: left: ε^{VTX} versus minimum transverse momentum, red is Monte-Carlo, blue is DATA; right: $\varepsilon^{DATA}/\varepsilon^{MC}$ versus minimum transverse momentum

4.1 The mixing angle and gluonium

The $\eta - \eta'$ mixing angle is one of the most interesting $SU(3)-$breaking hadronic parameters to measure since the $SU(3)$ symmetry was proposed. According to recent analysis in the context of Chiral Perturbation Theory, a description of the $\eta - \eta'$ system beyond leading order can be achieved in terms of just an angle only in the quark basis:

$$\begin{aligned} |\eta> &= X_\eta \frac{1}{\sqrt(2)}|u\bar{u} + d\bar{d}> + Y_\eta |s\bar{s}> \\ |\eta'> &= X_{\eta'} \frac{1}{\sqrt(2)}|u\bar{u} + d\bar{d}> + Y_{\eta'} |s\bar{s}> \end{aligned}$$

if we neglect possible gluonium admixture, we have $X_\eta = Y_{\eta'} = cos\varphi_P$ and $Y_\eta = -X_{\eta'} = sin\varphi_P$. As done in [6] and [5] the pseudo-scalar mixing angle in the flavor basis can be directly related to the ratio of the branching ratio of $\phi \to \eta'\gamma$ and $\phi \to \eta\gamma$. We use the Bramon approach [4] and [13], where the SU(3) breaking is taken into account via constituent quark mass ratio $m_s/\bar{m}$, and we take into account a correction induced by the OZI-rule, which reduce the VP wave-function overlaps [14], via the two parameters C_{NS} and C_S:

$$R = \frac{\mathrm{BR}(\phi \to \eta'\gamma)}{\mathrm{BR}(\phi \to \eta\gamma)} = cot^2\varphi_P \left(1 - \frac{m_s}{\bar{m}}\frac{C_{NS}}{C_S}\frac{tan\varphi_V}{sin2\varphi_P}\right)^2 \left(\frac{p_{\eta'}}{p_\eta}\right)^3 \tag{8}$$

Starting from our measurement $R = (4.77 \pm 0.09_{\mathrm{stat}} \pm 0.19_{\mathrm{sys}}) \cdot 10^{-3}$ we find as numerical solution to the problem:

$$\varphi_P = (41.4 \pm 0.3_{\mathrm{stat}} \pm 0.7_{\mathrm{sys}} \pm 0.6_{\mathrm{th}})^\circ \tag{9}$$

As done in [6], [5] the experimental error is evaluated using a Monte-Carlo extraction of R with a Gaussian distribution using as sigma the statistical error, and then evaluating the 68% confidence interval on φ_P. The same as been done for the systematic error: a Monte-Carlo extraction of R with a flat distribution, using $(R \pm \Delta R)$, is performed. We get a flat distribution for φ_P, from which we take the systematic.
The estimation of the theoretical uncertainties comes from the difference between angle extraction using the

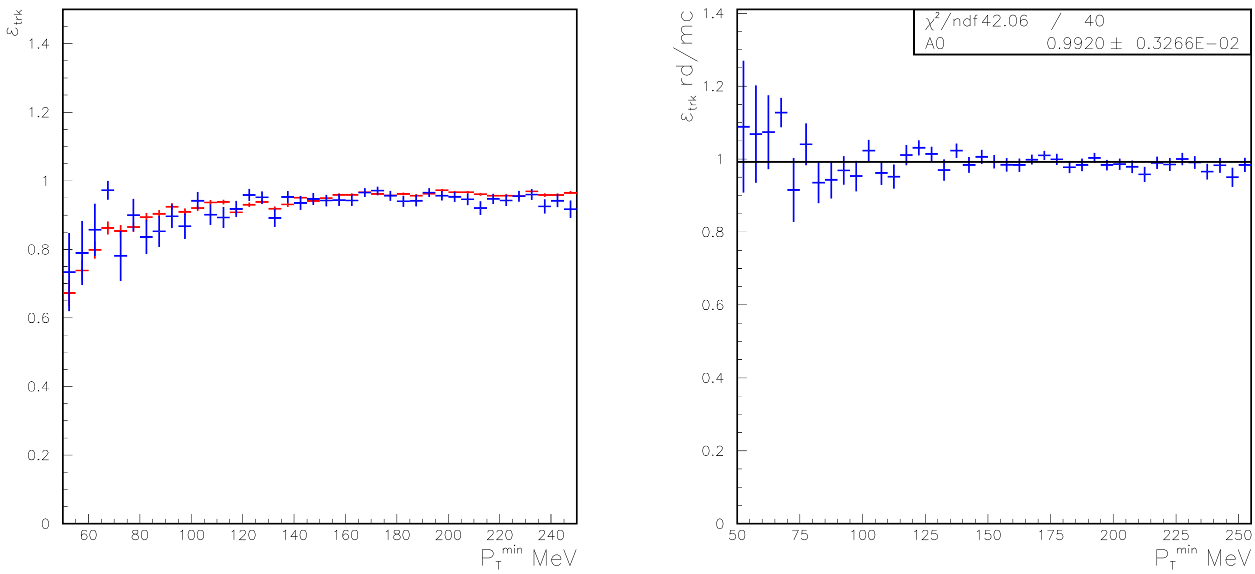

Figure 12: left: ε^{TRK} versus minimum transverse momentum, red is Monte-Carlo, blue is DATA; right: $\varepsilon^{DATA}/\varepsilon^{MC}$ versus minimum transverse momentum

values founded in literature for $m_s/\bar{m}$ (1.24 - 1.45), which is of the order $0.5°$, combined with the maximum variation observed changing the ratio of the two parameters $C_{NS} = 0.91 \pm 0.05$ and $C_S = 0.89 \pm 0.07$ within the theoretical error, that gives $0.3°$. The theoretical uncertainties is estimated to be $0.3° \oplus 0.5° = 0.6°$
The pseudo-scalar mixing angle in the flavor basis is related to the angle in the octet-singlet one, through the relation $\theta_P = \varphi_P - arctan\sqrt{2}$, then in the octet singlet basis our results becomes $\theta_P = (-13.3 \pm 0.3_{\text{stat}} \pm 0.7_{\text{sys}} \pm 0.6_{\text{th}})°$.

An interesting QCD test can be performed starting from the $\eta - \eta'$ mixing angle. The QCD involves quanta, the gluon's, which are expected to form bound states with one another, and mix with neutral mesons. While the η is well understood as an $SU(3)-$flavor octet with a small quarkonium singlet admixture, the η' is a good candidate to have a gluonium content.

If we allow for a η' gluonium content, we have to modify the equations which parametrize the physical states in the quark bases as the following:

$$|\eta> \;=\; X_\eta \frac{1}{\sqrt(2)} |u\bar{u} + d\bar{d}> + Y_\eta |s\bar{s}>$$
$$|\eta'> \;=\; X_{\eta'} \frac{1}{\sqrt(2)} |u\bar{u} + d\bar{d}> + Y_{\eta'} |s\bar{s}> + Z_{\eta'} |gluonium>$$

the $Z_{\eta'}$ parameter take in to account a possible mixing with glue. The parameter are normalized as:

$$X_\eta^2 + Y_\eta^2 = 1$$
$$X_{\eta'}^2 + Y_{\eta'}^2 + Z_{\eta'}^2 = 1$$

The relations with mixing angle became:

$$X_\eta = cos\varphi_P \qquad Y_\eta = -sin\varphi_P \tag{10}$$
$$X_{\eta'} = cos\phi_G sin\varphi_P \quad Y_{\eta'} = cos\phi_G cos\varphi_P \quad Z_{\eta'} = sin\phi_G \tag{11}$$

A possible gluonium content of the η' is revealed by

$$Z_{\eta'}^2 > 0 \Leftrightarrow X_{\eta'}^2 + Y_{\eta'}^2 < 1 \tag{12}$$

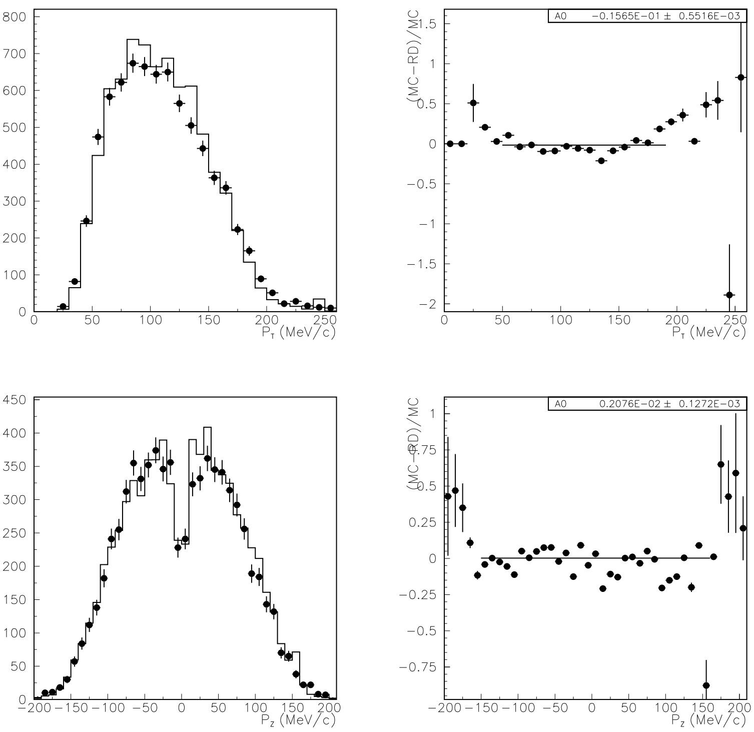

Figure 13: MC-DATA comparison on P_T (up) and P_Z (down) for charged tracks

Let me stress that in this case the mixing angle cannot be extracted in simple way. We can use constraints on $X_{\eta'}$ and $Y_{\eta'}$ obtained in a nearly model independent way using simple $SU(3)$ ideas, exploiting the magnetic dipole nature of the transition $VP\gamma$ and $PV\gamma$ and evaluating ratios of branching ratios in order to normalize to one common coupling constant. Using the Wess-Zumino-Witten term of the chiral Lagrangian we can evaluate the coupling to two photons.

We will use the following constraints

$$\frac{\Gamma(\eta' \to \rho\gamma)}{\Gamma(\omega \to \pi^0\gamma)} = C \cdot 3 \left(\frac{m_{\eta'}^2 - m_\rho^2}{m_\omega^2 - m_\pi^2} \frac{m_\omega}{m_{\eta'}} \right)^3 X_{\eta'}^2 \tag{13}$$

$$\frac{\Gamma(\eta' \to \gamma\gamma)}{\Gamma(\pi^0 \to \gamma\gamma)} = \frac{1}{9} \left(\frac{m_{\eta'}}{m_\pi} \right)^3 (5X_{\eta'} + \sqrt{2}\frac{f_q}{f_s} Y_{\eta'})^2 \tag{14}$$

$C = C_{NS}/cos\varphi_V$ is a correction induced by the OZI-rule to reduce the VP wave-function overlaps [14]. In the hypotheses of no gluonium content we have $Z_{\eta'} = sin\phi_G = 0$ and $cos\phi_G = 1$:

$$|Y_{\eta'}| = cos\varphi_P \tag{15}$$

this is also a reasonable approximation if the mixing with gluonium is small. The constraints on the $X_{\eta'}$ and $Y_{\eta'}$ parameter induced by the previous relations are shown in fig.17. Again as we have done in [5], we extract $Z_{\eta'}^2 = 1 - X_{\eta'}^2 - Y_{\eta'}^2$ from the three quantities $X_{\eta'}$, $Y_{\eta'}$ and $|X_{\eta'} + \frac{\sqrt{2}}{5}\frac{f_q}{f_s}Y_{\eta'}|$ in three correlated ways. We built a χ^2 which, minimized, gives $Z_{\eta'}^2$ while $\chi^2 + 1$ bound gives the error. We get

$$X_{\eta'}^2 + Y_{\eta'}^2 = 0.92 \pm 0.06 \tag{16}$$

The error on this parameters is dominated by the ones of the constraint due to $\Gamma(\eta' \to \gamma\gamma)/\Gamma(\pi^0 \to \gamma\gamma)$ and $\Gamma(\eta' \to \rho\gamma)/\Gamma(\omega \to \pi^0\gamma)$ see tab.(5). Another constraint was suggested by Kou [16] and is based on the

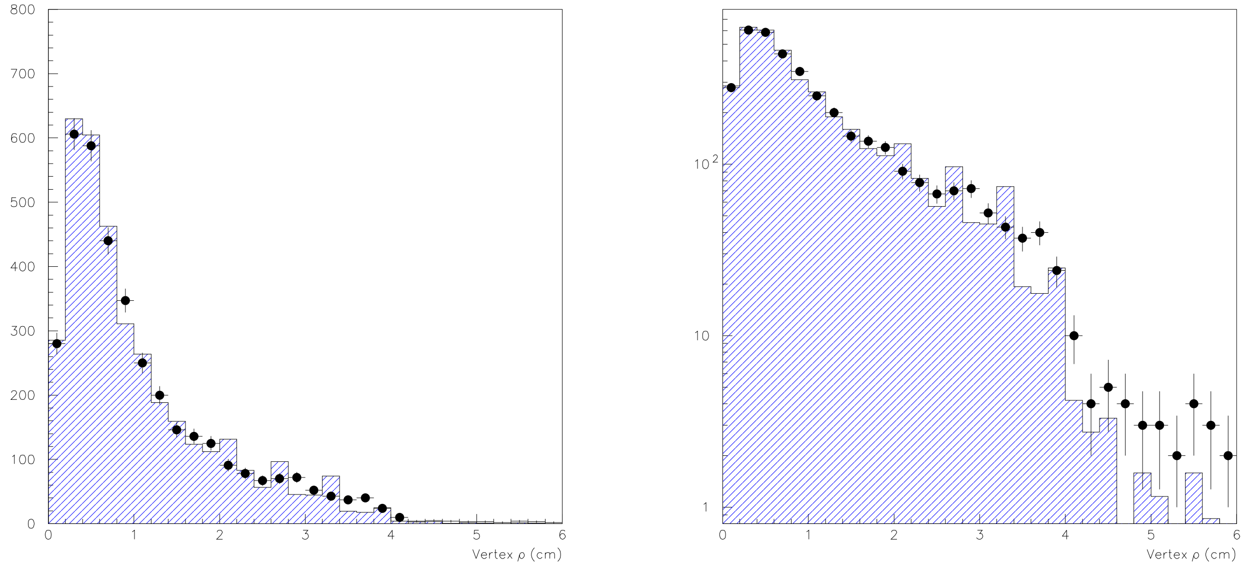

Figure 14: MC-DATA comparison on charged vertex; ρ

Quantity	value
$\lvert X_{\eta'} + \frac{\sqrt{2}}{5}\frac{f_q}{f_s} Y_{\eta'}\rvert$	0.75 ± 0.02
$\lvert X_{\eta'}\rvert$	0.60 ± 0.04
$\lvert Y_{\eta'}\rvert$	$0.750 \pm 0.004 \pm 0.008$

Table 4: Constraints on coefficients in quark basis for the η' [13]

$\eta' \to \omega\gamma$ decay. Applying again the correction from [14] we obtain the following relation:

$$\frac{\Gamma(\eta' \to \omega\gamma)}{\Gamma(\omega \to \pi^0\gamma)} = \frac{1}{3}\left(\frac{m_{\eta'}^2 - m_\omega^2}{m_\omega^2 - m_\pi^2}\frac{m_\omega}{m_{\eta'}}\right)^3 \left[C_{NS} \cdot X_{\eta'} + 2\frac{m_s}{\bar{m}} C_S \cdot tan\varphi_V \cdot Y_{\eta'}\right]^2 \tag{17}$$

and the relation between $X_{\eta'}$ and $Y_{\eta'}$ gives $|X_{\eta'} + 2\frac{m_s}{\bar{m}}\frac{C_S}{C_{NS}} \cdot tan\varphi_V \cdot Y_{\eta'}| = 0.63 \pm 0.09$.
In figure.18.up we show the new constraint suggested by Kou. The present experimental value give no improvement about gluonium content, we should like reduce the band due to the new constraint. The main contribution to the error comes from $\Gamma(\eta' \to \omega\gamma)$, which has a relative error of 18%. We could reduce this error to 8% measuring the $BR(\eta' \to \omega\gamma)$ (his value is $(3.03 \pm 0.31)\%$ [17]), analyzing the data used in this analysis, in the hypothesis of a selection efficiency at level of 20% and neglecting any systematics. In figure.18.down we show the possible scenario with the new measurement, if the mean value of the $BR(\eta' \to \omega\gamma)$ doesn't

Quantity	value
$\Gamma(\eta' \to \gamma\gamma)/\Gamma(\pi^0 \to \gamma\gamma)$	547.5 ± 43.5
$\Gamma(\eta' \to \rho\gamma)/\Gamma(\omega \to \pi^0\gamma)$	$(79 \pm 7) \cdot 10^{-3}$
$\Gamma(\phi \to \eta'\gamma)/\Gamma(\phi \to \eta\gamma)$	$(4.77 \pm 0.22) \cdot 10^{-3}$
$\Gamma(\eta' \to \omega\gamma)/\Gamma(\omega \to \pi^0\gamma)$	82 ± 11

Table 5: Experimental value for the radiative processes under study

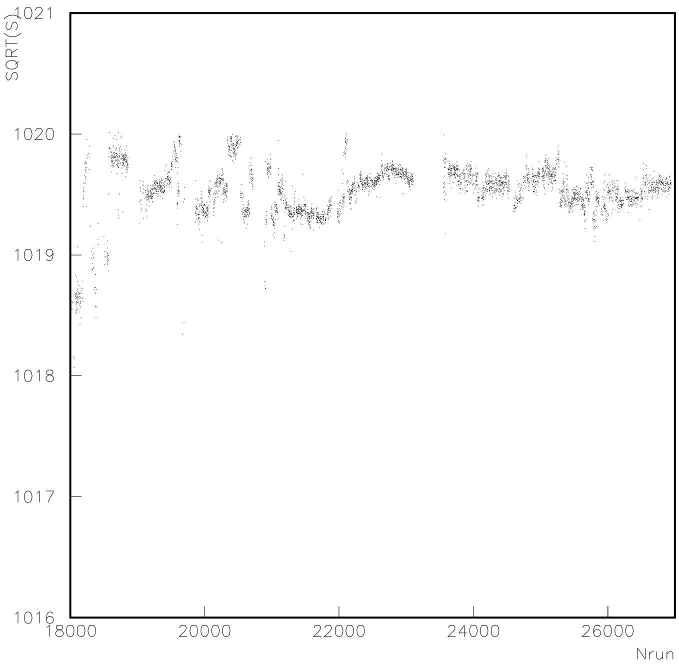

Figure 15: square root of s versus run number

change. The new constraint could give new information on the gluonium content of the η', so it seems very interesting to perform this measurement.

4.1.1 Gluon mixing measurement

In this section we evaluate the $Z^2_{\eta'}$ value from the same constraints, introduced in the previous section, expressing all the relation as function of the pseudoscalar mixing angle and the gluon mixing angle ϕ_G. We build a χ^2 function and we solve the problem with and without glonium.

If we allow for gluonium content the ratio $R = \mathrm{B}R(\phi \to \eta'\gamma)/\mathrm{B}R(\phi \to \eta\gamma)$ can be written as:

$$\frac{\mathrm{B}R(\phi \to \eta'\gamma)}{\mathrm{B}R(\phi \to \eta\gamma)} = \cot^2 \varphi_P \cos^2 \phi_G \left(1 - \frac{m_s}{\bar{m}} \frac{C_{NS}}{C_S} \frac{\tan \varphi_V}{\sin 2\varphi_P}\right)^2 \left(\frac{p_{\eta'}}{p_\eta}\right)^3 \tag{18}$$

Expressing all the formulas in term of the two angles φ_P and ϕ_G, we have:

$$\frac{\Gamma(\eta' \to \rho\gamma)}{\Gamma(\omega \to \pi^0\gamma)} = C \cdot 3 \left(\frac{m^2_{\eta'} - m^2_\rho}{m^2_\omega - m^2_\pi} \frac{m_\omega}{m_{\eta'}}\right)^3 \sin^2 \varphi_P \cos^2 \phi_G \tag{19}$$

$$\frac{\Gamma(\eta' \to \gamma\gamma)}{\Gamma(\pi^0 \to \gamma\gamma)} = \frac{1}{9} \left(\frac{m_{\eta'}}{m_\pi}\right)^3 \cos^2 \phi_G (5 \sin \varphi_P + \sqrt{2} \frac{f_q}{f_s} \cos \varphi_P)^2 \tag{20}$$

We build a χ^2 function to combine the three constraints; we have three experimental input:

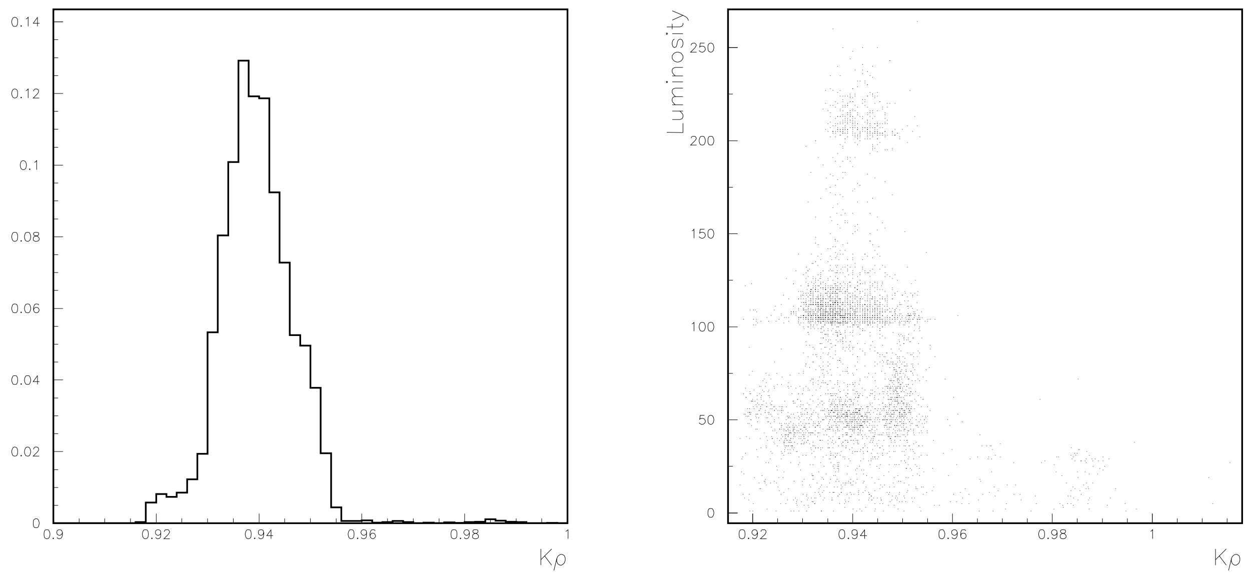

Figure 16: left: corrections due to interference weighted for run luminosity; right: corrections versus run luminosity

$y_1 = \Gamma(\eta' \to \gamma\gamma)/\Gamma(\pi^0 \to \gamma\gamma)$, $y_2 = \Gamma(\eta' \to \rho\gamma)/\Gamma(\omega \to \pi^0\gamma)$ and $y_3 = R_\phi$ (see table.5), and three functions:

$$y_1^{th} = \frac{1}{9}\left(\frac{m_{\eta'}}{m_\pi}\right)^3 (5\cos\phi_G \sin\varphi_P + \sqrt{2}\frac{f_q}{f_s}\cos\phi_G\cos\varphi_P)^2$$

$$y_2^{th} = \frac{C_{NS}}{\cos\varphi_V}\cdot 3\left(\frac{m_{\eta'}^2 - m_\rho^2}{m_\omega^2 - m_\pi^2}\frac{m_\omega}{m_{\eta'}}\right)^3 \cos^2\phi_G \sin^2\varphi_P$$

$$y_3^{th} = \cot^2\varphi_P\cos^2\phi_G\left(1 - \frac{m_s}{\bar{m}}\frac{C_{NS}}{C_S}\frac{\tan\varphi_V}{\sin 2\varphi_P}\right)^2\left(\frac{p_{\eta'}}{p_\eta}\right)^3$$

The functions y_i^{th} depend from some parameters, $y_i^{th}(\cos^2\phi_G, \cos^2\varphi_P; P_j)$, with $P_j = f_s, f_q, C_{NS}, C_S, \frac{m_s}{\bar{m}}$ and we look for a solution as $(\cos^2\phi_G, \cos^2\varphi_P)$; we use the values from the table 6 and we suppose no correlation between the parameters.

Table 6: The values of the fixed parameters are from [2], the first two, and from [14] the others.

Parameter	f_q	f_s	C_{NS}	C_S	$\frac{m_s}{\bar{m}}$
Value	1 ± 0.01	1.4 ± 0.014	0.91 ± 0.05	0.89 ± 0.07	1.24 ± 0.07

The χ^2 is defined as follows:

$$\chi^2 = \Sigma_{i,j=1,3}\left(y_i - y_i^{th}\right) \times V_{ij}^{-1}\left(y_j - y_j^{th}\right)$$

V_{ij} is the error matrix which is a function of theoretical uncertainties, as well as the experimental errors:

$$V_{ij} = [B_{ij} + (A_{ik} \times C_{kl} \times A_{lj}^T)]$$

where

$$B_{ij} = \begin{pmatrix} \sigma^2_{y_1} & 0 & 0 \\ 0 & \sigma^2_{y_2} & 0 \\ 0 & 0 & \sigma^2_{y_3} \end{pmatrix} ; A_{ik} = \begin{pmatrix} \frac{\partial y_1^{th}}{\partial f_s} & \frac{\partial y_1^{th}}{\partial f_q} & \frac{\partial y_1^{th}}{\partial C_{NS}} & \frac{\partial y_1^{th}}{\partial C_S} & \frac{\partial y_1^{th}}{\partial \frac{m_s}{\bar{m}}} \\ \frac{\partial y_2^{th}}{\partial f_s} & \frac{\partial y_2^{th}}{\partial f_q} & \frac{\partial y_2^{th}}{\partial C_{NS}} & \frac{\partial y_2^{th}}{\partial C_S} & \frac{\partial y_2^{th}}{\partial \frac{m_s}{\bar{m}}} \\ \frac{\partial y_3^{th}}{\partial f_s} & \frac{\partial y_3^{th}}{\partial f_q} & \frac{\partial y_3^{th}}{\partial C_{NS}} & \frac{\partial y_3^{th}}{\partial C_S} & \frac{\partial y_3^{th}}{\partial \frac{m_s}{\bar{m}}} \end{pmatrix}$$

and

$$C_{kl} = \begin{pmatrix} \sigma^2_{f_s} & 0 & 0 & 0 & 0 \\ & \sigma^2_{f_q} & 0 & 0 & 0 \\ & & \sigma^2_{C_{NS}} & 0 & 0 \\ & & & \sigma^2_{C_S} & 0 \\ & & & & \sigma^2_{\frac{m_s}{\bar{m}}} \end{pmatrix}$$

the matrix C_{kl} is diagonal because we suppose no correlation between the parameters.

The solution to the problem in the hypothesis of no gluonium, $Z^2 = 0$ i.e. $\cos^2\phi_G = 1$, is $\varphi_P = (41.2^{+1.8}_{-0.5})^\circ$; the χ^2 quality is bad, $\chi^2/N.d.f. = 10.89/2$, this suggest to exploit possible non zero value for Z^2.
The solution to the problem with gluonium is the couple: $\varphi_P = (39.8 \pm 0.8)^\circ$ and $|\phi_G| = (21 \pm 3)^\circ$ this imply $Z^2 = 0.13 \pm 0.04$. In this case the quality of the χ^2 is excellent, $\chi^2/N.d.f. = 0.00126/1$ with a $P(\chi^2/N.d.f.) = 0.97$.
The same solutions come from the minimization of the χ^2 which include the correlations between the experimental measurement y_1 and y_2, $r_{1,2} = -12\%$ as from [17]; the matrix about the experimental contributions becomes:

$$B_{ij} = \begin{pmatrix} \sigma^2_{y_1} & cov(y_1 y_2) & 0 \\ cov(y_1 y_2) & \sigma^2_{y_2} & 0 \\ 0 & 0 & \sigma^2_{y_3} \end{pmatrix}$$

the χ^2 decrease and $P(\chi^2/N.d.f.)$ go up to 0.99. We find a Z^2 value compatible with three sigma existence of gluonium.
In the fig.19 we plot the constraints in the plain Z^2, φ_P with a fourth constraint, as suggested by Kou [16], based on the $\eta' \to \omega\gamma$ decay. We include the fourth constraint from (17), $y_4 = \Gamma(\eta' \to \omega\gamma)/\Gamma(\omega \to \pi^0\gamma)$ in our χ^2:

$$\chi^2 = \Sigma_{i,j=1,4} \left(y_i - y_i^{th}\right) \times (V'_{ij})^{-1} \left(y_j - y_j^{th}\right)$$

with

$$y_4^{th} = \frac{1}{3}\left(\frac{m^2_{\eta'} - m^2_\omega}{m^2_\omega - m^2_\pi}\frac{m_\omega}{m_{\eta'}}\right)^3 \left[C_{NS} \cdot \cos\phi_G \sin\varphi_P + 2\frac{m_s}{\bar{m}} C_S \cdot \tan\varphi_V \cdot \cos\phi_G \cos\varphi_P\right]^2$$

The error matrix $(V'_{ij}) = [B'_{ij} + (A'_{ik} \times C_{kl} \times (A'_{lj})^T)]$ includes correlations between the experimental value of y_1 and y_2 and y_4 in the matrix $B'_{ij} = cov(y_i, y_j)$, which is not diagonal: correlation between 1 and 2 is $r_{12} = -12\%$, between 1 and 4 is $r_{14} = +8\%$ and between 2 and 4 $r_{24} = -24\%$ [17]: the matrix about experimental errors becomes:

$$B'_{ij} = \begin{pmatrix} \sigma^2_{y_1} & cov(y_1 y_2) & 0 & cov(y_1 y_4) \\ cov(y_1 y_2) & \sigma^2_{y_2} & 0 & cov(y_2 y_4) \\ 0 & 0 & \sigma^2_{y_3} & 0 \\ cov(y_1 y_4) & cov(y_2 y_4) & 0 & \sigma^2_{y_4} \end{pmatrix}.$$

The solution in the hypothesis of no gluonium, which means $\cos^2\phi_G = 1$ is $\varphi_P = (41.5^{+0.6}_{-0.7})^\circ$. The χ^2 quality is bad, $\chi^2/N.d.f. = 11.34/3$, with a $P(\chi^2/N.d.f.) = 0.01$ and suggest again to exploit possible non zero value for Z^2.

Allowing for gluonium, we obtain $\chi^2/N.d.f. = 1.419/2$ with a $P(\chi^2/N.d.f.) = 0.49$. The final result does not change significantly compared with the one from the χ^2 with three constraints, here we get: $\varphi_P = (39.7 \pm 0.7)^\circ$ and $Z^2 = 0.14 \pm 0.04$, $|\phi_G| = (22 \pm 3)^\circ$; we have a Z^2 slightly grather than the one from the three constraints.

5 Conclusion

We present the first observation of $\phi \rightarrow \eta'\gamma$ with $\pi^+\pi^-7\gamma$ final state; we analyzed about $427\,pb^{-1}$ of integrated luminosity collected by KLOE at the DAϕNE collider. We reduce the error on the determination of the BR and using its ratio with the BR of $\phi \rightarrow \eta\gamma$ we obtain the best determination of the pseudoscalar mixing angle. We also extract the pseudoscalar mixing angle parameter in the hypothesis of gluonium content and we find $Z^2 = 0.14 \pm 0.04$ and $\varphi_P = (39.7 \pm 0.7)^\circ$.

Acknowledgments

I would like to thank very much Simona Giovannella and Paolo Gauzzi, with Fabio Ambrosino and Giorgio Capon for their big help in the devolopment of the work and for their useful suggestions.
Many thanks to Rafel Escribano for his suggestions about pseudoscalar mixing angle and evaluation of gluonium and to Gianluca Imbriani for his help in the χ^2 analysis for gluonium evaluation.

References

[1] R. Kaiser and H. Leutwyler, hep-ph/9806336

[2] T. Feldmann, *Int. Jou. Mod. Phys.* A15, 159 (2000)

[3] C. Becchi and G. Morpurgo *Phys. Rev.* 140, B687 (1965)

[4] A. Bramon, R. Escribano and M.D. Scadron *Eur. Phys. J.* C7, 271 (1999)

[5] A. Aloisio et al., *Measurement of* $\Gamma(\phi \to \eta'\gamma)/\Gamma(\phi \to \eta\gamma)$ *and the pseudoscalar mixing angle*, *Phys.Lett.* B541:45-51,2002

[6] F. Ambrosino, *Analysis of* $\phi \to \eta'\gamma$, $\phi \to \eta\gamma$ *in* $\pi^+\pi^-\gamma\gamma\gamma$ *final state*, KLOE memo n.266/02

[7] C. Di Donato, *Study on* $\phi \to \eta'\gamma$ *with seven* γ *and two tracks final state*, KLOE memo n.268/02

[8] E. Ramberg et al., FNAL E731 Coll. *PRL 70* 2525 (1993)

[9] F. Perfetto, Thesis Degree *Esperimento KLOE a DAFNE: Studio del decadimento del mesone* η *in pioni neutri*, 2003

[10] S. Giovannella and S. Miscetti "*Measurement of BR(*$\phi \to \pi^0\pi^0\gamma$*) with 2000 Data*" KLOE note 178 April 2002

[11] C. Di Donato, *A minimum bias EVCL for* ϕ *radiative decays*, KLOE memo n.306/05

[12] M. Martini, S. Miscetti, *Determination of the probability of accidental coincidence between machine background and collision events and fragmentation of electromagnetic showers*, Kloe Note n.201/05

[13] J.L. Rosner *Phys. Rev.* D27, 1101 (1983)

[14] A. Bramon, R. Escribano and M.D. Scadron *Phys. Lett.* B 503, 271 (2001)

[15] S. Giovannella, S. Miscetti and G. Capon, F. Ambrosino; *Private comunication*

[16] E. Kou *PRD* 63, 54027 (2001)

[17] *Review of Particle Physiscs 2006 J. Phys G: Nucl. Part. Phys.* 33 (2006) 1

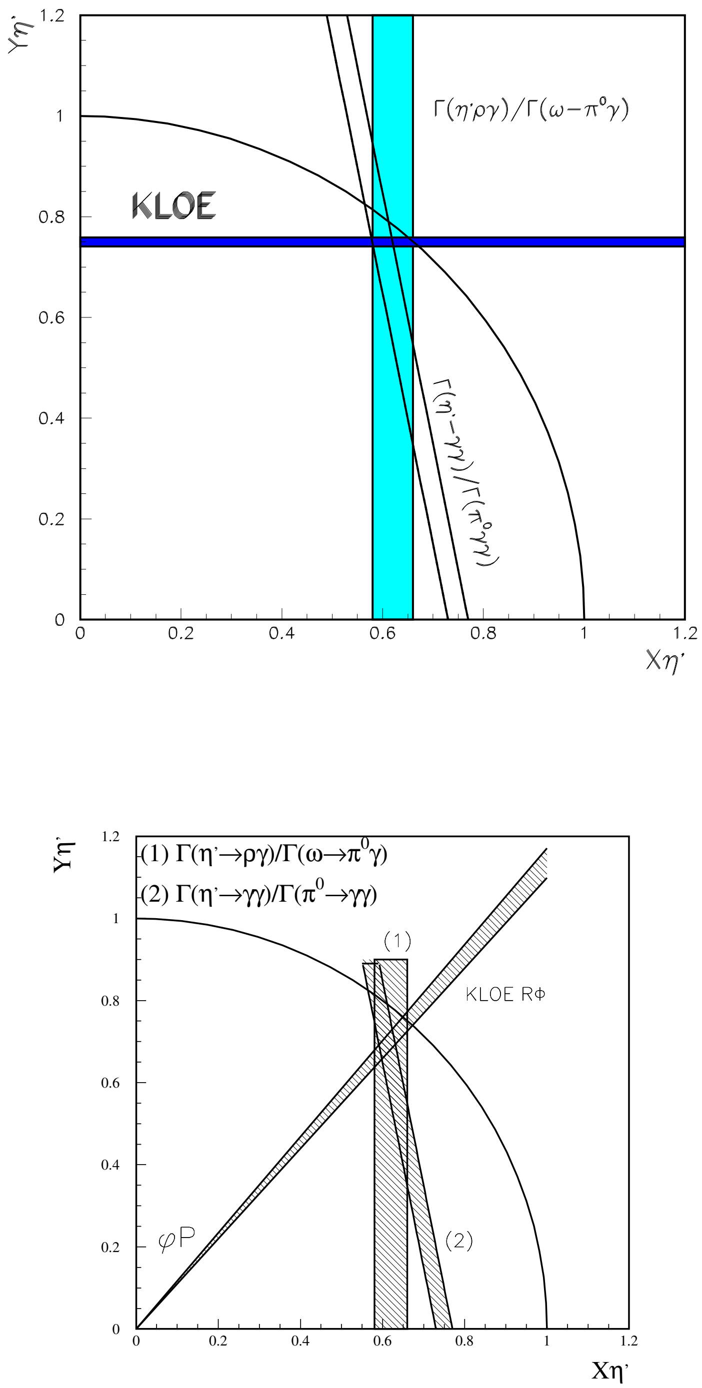

Figure 17: Bounds on X and Y: $\frac{\Gamma(\eta'\to\gamma\gamma)}{\Gamma(\pi^0\to\gamma\gamma)}$: $|X_{\eta'} + \frac{\sqrt{2}}{5}\frac{f_q}{f_s}Y_{\eta'}| = 0.75 \pm 0.02$; $\frac{\Gamma(\eta'\to\rho\gamma)}{\Gamma(\omega\to\pi^0\gamma)}$: $|X_{\eta'}| = 0.60 \pm 0.04$. Left: $\frac{\Gamma(\phi\to\eta'\gamma)}{\Gamma(\phi\to\eta\gamma)}$: $|Y_{\eta'}| = 0.750 \pm 0.004 \pm 0.008$; Right: $\frac{\Gamma(\phi\to\eta'\gamma)}{\Gamma(\phi\to\eta\gamma)}$: $\arctan(X_{\eta'}/Y_{\eta'}) = (41.4 \pm 0.3 \pm 0.7)^\circ$.

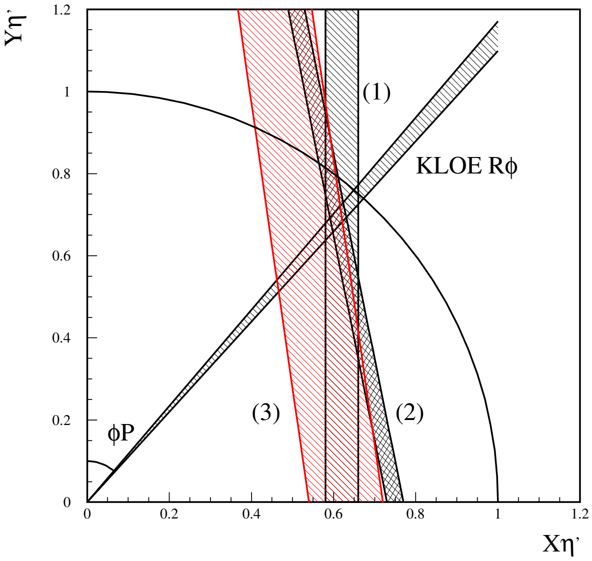

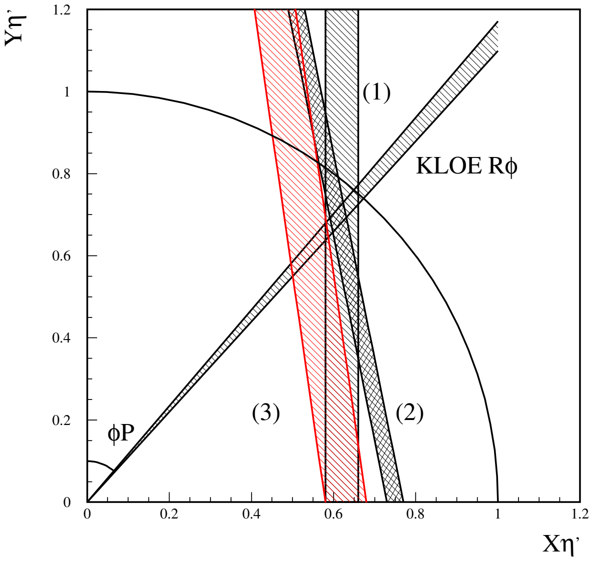

Figure 18: Bounds on X and Y: (1) $\to \Gamma(\eta' \to \rho\gamma)/\Gamma(\omega \to \pi^0\gamma)$, (2) $\to \Gamma(\eta' \to \gamma\gamma)/\Gamma(\pi^0 \to \gamma\gamma)$ and (3) $\to \Gamma(\eta' \to \omega\gamma)/\Gamma(\omega \to \pi^0\gamma)$; Up: red line shows the constraint due to $\eta' \to \omega\gamma$ decay using $\Gamma(\eta' \to \omega\gamma)$ as from [17]; Down: as in the previous plot but we reduce the error on $\Gamma(\eta' \to \omega\gamma)$ up to 8%

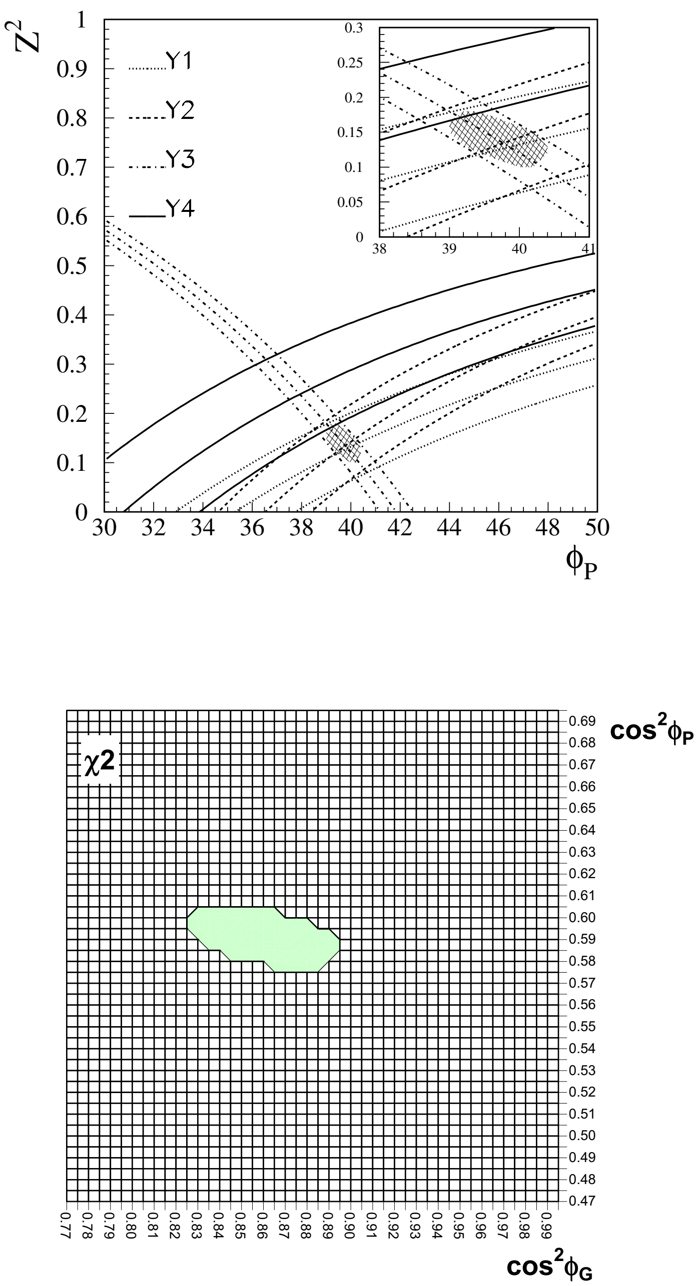

Figure 19: Up: the four constraint in the Z^2, φ_P plain, $y_1 = \Gamma(\eta' \to \gamma\gamma)/\Gamma(\pi^0 \to \gamma\gamma)$, $y_2 = \Gamma(\eta' \to \rho\gamma)/\Gamma(\omega \to \pi^0\gamma)$ $y_3 = R_\phi$ and $y_4 = \Gamma(\eta' \to \omega\gamma)/\Gamma(\omega \to \pi^0\gamma)$; the 68% C.L. region for Z^2 and φ_P is shown. Down: The region shows the 68% C.L. solutions in the $\cos^2\phi_G, \cos^2\varphi_P$ plain from the minimization of $\chi^2 = \Sigma_{i,j=1,4}\left(y_i - y_i^{th}\right) \times V_{ij}^{-1}\left(y_j - y_j^{th}\right)$, V_{ij} is the error matrix which is a function of theoretical uncertainties, as well as the experimental errors